

Statistical mechanics of two-dimensional domain walls

S. T. Chui

Bartol Research Foundation of The Franklin Institute,
University of Delaware, Newark, Delaware 19711

(Received 11 December 1980)

The statistical mechanics of two classes of two-dimensional domain walls including the honeycomb structure is discussed. Particular attention is focused on their structure factors, free energies, and phonon dispersion relationships. Relevance of these to recent developments on the commensurate-incommensurate transition is pointed out. The possibility of a dislocation unbinding transition in the incommensurate phase close to the commensurate-incommensurate transition is discussed.

I. INTRODUCTION

Recent work in the commensurate-incommensurate transition (CIT) has revived interests in the statistical mechanics of domains walls. These walls are created at the onset and characterize the nature of the incommensurate phase. A model of a *one-dimensional* array of domain walls (see Fig. 1) (called the "striped phase") was discussed by a number of authors recently¹ using a path integral method first discussed by de Gennes in the context of polymers.² While this model may under some instances be the experimentally relevant one,³ a *two-dimensional* network of domain boundaries seems to have been observed in experiments involving various rare gases on graphite.⁴ There are two different classes of two-dimensional domain walls that have been discussed. The first class, which we call type *A*, is a straightforward generalization of the striped phase and consists of intersecting stripes such that the statistical mechanics of one kind of stripes is independent of that of the other kind [see, for example, Fig. 2(a)]. There is an energy of intersection (E_0) of the stripes of course but this energy is independent of the fluctuation of the stripes. This has been discussed recently by a number of authors.⁵ The type-*A* domain walls differ topologically from the honeycomb struc-

ture [see Fig. 2(b)], which is predicted⁶ to be the zero-temperature configuration for rare gases on graphite. The statistical mechanics of this type of domain boundaries (type *B*) has not been looked at and is the main focus of the present paper.

Let us review briefly some of the results for the striped phase. From now on we shall use the notation of the CIT even though domain boundaries can

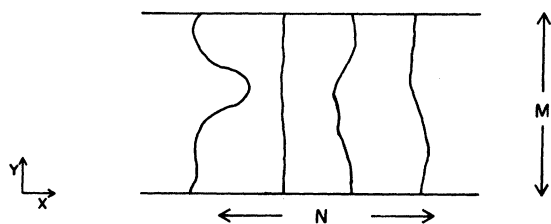


FIG. 1. A schematic illustration for a one-dimensional array of domain boundaries (the striped phase).

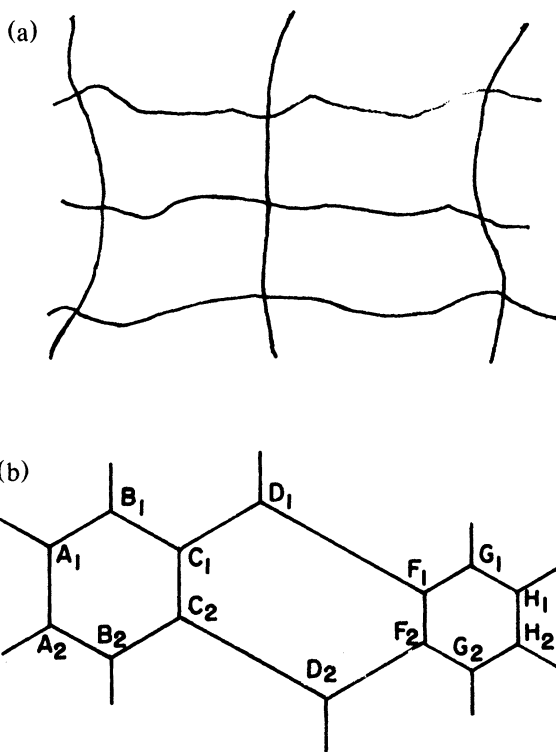


FIG. 2. (a) Type-*A* domain boundaries. Note that it just consists of crossing stripes. (b) Type-*B* domain boundaries.

occur in different contexts and our treatment will be applicable to those situations as well. Most models of the CIT approximates the epitaxy as an isotropic elastic medium with an atomic spacing a in a periodic static two-dimensional external potential of period b exerted by the substrate.⁷ For the striped phase, the x and the y coordinates are assumed to be decoupled. At $T=0$, for a large enough difference in the spacing $b-a$, a CIT will take place with the creation of domain boundaries (misfit dislocations). These domain boundaries interact with each other with short-range potential of the form $A \exp(-Br)$, where A, B are constants and r is the distance between them. Because the repulsion is exponentially short ranged, the equilibrium interwall spacing l is a logarithmic function of $b-a$. The phonon spectrum has also been worked out⁷ and is shown schematically in Fig. 3(a). It consists of a linear gapless part with a sound velocity c proportional to $\exp(-Bl)$ plus an optical branch with a gap. The acoustic branch comes from the collective motion of the domain boundaries, hence the form $\exp(-Bl)$. Note that c is extremely small at large l . This should be contrasted with the phonon dispersion in the commensurate case, illustrated in Fig. 3(b), which has a gap.

The physics is quite different at finite temperatures for the striped phase. The domain boundaries can wander and bend, the effective range of their mutual interaction is increased. The statistical mechanics of this problem can be treated by the path integral (or transfer matrix) technique in which each wall is viewed as a phase-space trajectory of a quantum particle. The mathematics is recapitulated in Appendix A where some new results and some of the subtleties are also presented. (For example, most previous treatments force the quantum particles to be fermions, this is actually not necessary even though it makes little difference to the final result.) The results are summarized in Table I. The dependence of the density of domain walls ($1/l$) on $b-a$ has been much emphasized in the past and will not be belabored here. There are some interesting facts that have escaped attention, however. The phonon spectrum now exhibits no gap separating the optical and acoustic branch. Furthermore, the sound velocity is drastically changed. It goes to zero much more slowly as the CIT is approached. Instead of proportional to $\exp(-Bl)$ it is proportional to $\sqrt{1/l}$ ($l \rightarrow \infty$ as the CIT is approached). This is illustrated in Fig. 3(c). The density autocorrelation function, which exhibits a δ -function peak at $T=0$, becomes much broader at $T \neq 0$. Previous calculations,² assuming only a hard-core potential between the walls, indicates that the wall autocorrelation function $C(q)$ exhibits a weak logarithmic divergence of the form $(C/T) \ln[(q-2\pi/l)/2\pi/l]$. As we discussed in the Appendix, when the residual short-range interactions $\bar{V} = Ae^{-Ba}$ between the walls are included, $C(q)$ ex-

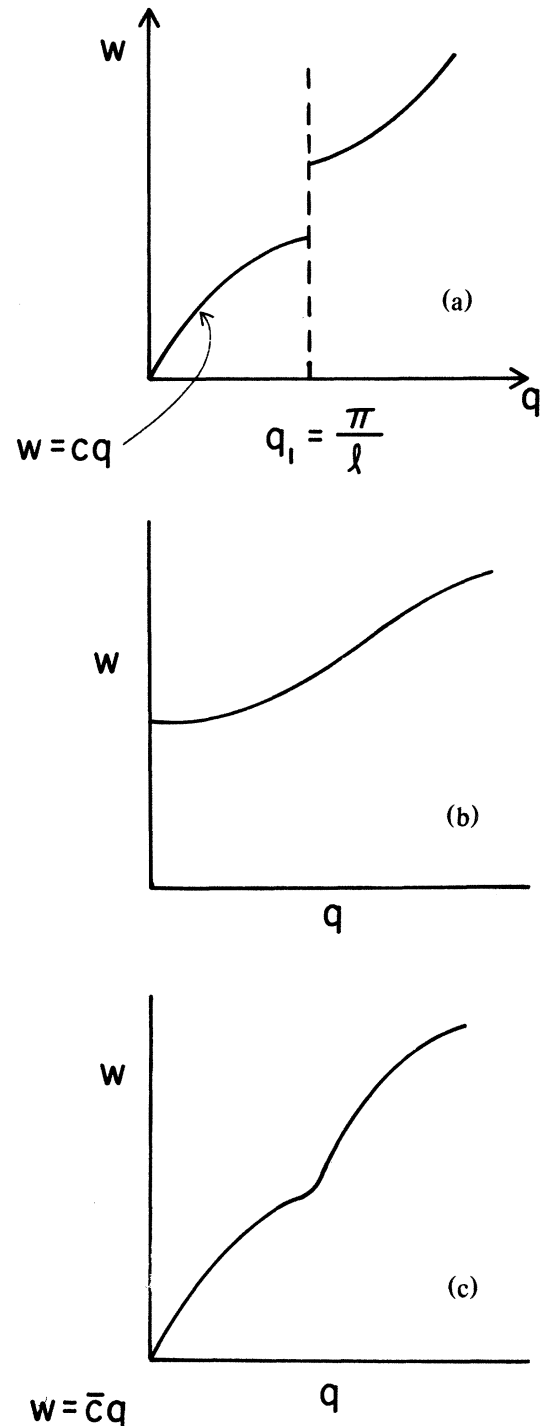


FIG. 3. (a) A frequency vs wave vector plot for phonons in an incommensurate phase at zero temperature. (b) A frequency vs wave vector plot for phonons in a commensurate phase. Note the existence of the gap at $q=0$. (c) A frequency vs wave vector plot for phonons in an incommensurate phase at finite temperature. Note that \bar{c} is much larger than c . Note also that there is no gap separating the optical from the acoustic branch.

TABLE I. A table summarizing the functional dependences of the physical properties of different classes of domain boundaries on its density or distance away from the CIT.

	Striped phase or type-A boundaries		Type-B boundaries	
	$T=0$	$T \neq 0$	$T=0$	$T \neq 0$
Average spacing l	$\ln \frac{b-a}{b}$	$\left(\frac{b-a}{a}\right)^{1/2}$	$\left(\frac{b-a}{a}\right)$	First order or $\left(\frac{b-a}{a}\right)$
The sound velocity of the epitaxy	$\exp(-Bl)$	$\sqrt{l/l}$	$\sqrt{l/l}$	$\sqrt{l/l}$
Density autocorrelation function of the domain walls $C(q)$	$\delta\left(q - \frac{2\pi}{l}\right)$	$\ln\left[-\frac{2\pi}{l}\right]$ (hard core) $\left[q - \frac{2\pi}{l}\right]^\alpha$ (short-range repulsion) α defined in Eq. (1)	$\delta\left(q - \frac{2\pi}{l}\right)$	A gap now exists
Structure factor $S(q)$ of the epitaxy near $q = \frac{2\pi}{l}$	$\delta(q - q_0)$	$(q - q_0)^\beta$ β defined in Eq. (4)	$\delta(q - q_0)$	$S(q) = \frac{2\mu}{\delta q^2 + \mu^2} f(\delta q)$ $+ \frac{\sin \delta q / \mu}{\delta q} g(\delta q)$ $f(\delta q) \rightarrow 0$ as $l \rightarrow 0$ $\mu = \frac{1}{(\beta \gamma a + l/2)}$ See Eq. (16) for details.

hibits a power-law divergence of the form

$$\frac{C}{\alpha T} \left[\left(\frac{q_x - \frac{2\pi}{d}}{\frac{2\pi}{d}} \right)^\alpha - 1 \right] \quad \text{when } \frac{q_x - 2\pi/d}{2\pi/d} \ll 1.$$

α is approximately given by

$$\alpha = \begin{cases} \frac{2}{\pi} \sin \pi(1 - 1/l) \bar{V}/\gamma a^2 & \text{when } \bar{V}/\gamma \ll 1 \\ 2[1 - \exp[-(2 - 2/l)]] & \text{when } \bar{V}/\gamma \gg 1 \end{cases} \quad (1)$$

Here γ is the elastic modulus of the walls. [See Eq. (A1) for a precise definition.] Note that at the onset of the CIT the above divergence is significant only over a very narrow range of q . The structure factor $S(q)$ of the epitaxial atoms is not simply relat-

ed to $C(q)$ however. As is indicated by Villain¹

$$S(\delta q + q_0) = \int_{-\infty}^{\infty} dx e^{ix\delta q} \exp F(x), \quad (2)$$

where q_0 is the position of the Bragg peak. For the striped phase, $q_0 = (2\pi/a(1 + 1/l), 0)$. $F(x)$ is related to the equal time correlation function of the domain walls by

$$F(x) = -q_0^2 z^2 \int_0^x d(u - u') l \langle \delta \rho(u) \delta \rho(u') \rangle \\ = \frac{4}{N^2} \int \sin^2(qx/2) \langle \delta \rho_q \delta \rho_{-q} \rangle / q^2, \quad (3)$$

where $\delta \rho$ is the change in the number of walls at position u , viz., $\delta \rho = \rho - \langle \rho \rangle$; $\rho(u) = \sum \delta(u - x_i)$. z is the net displacement caused by a single domain wall. Unlike $C(q)$, the singular behavior of $F(x)$ and hence $S(q)$ is unaffected when the short-range repulsion between the walls is introduced because it is dominated by the correlation function $\langle \delta \rho_q \delta \rho_{-q} \rangle$ for

small q ; the singular behavior of the latter is not affected by the short-range repulsion. As is shown in Ref. 1, S exhibits a power-law behavior with an exponent

$$\beta = -1 + b^2/2\pi^2 a^2 . \quad (4)$$

Let us next turn our attention to two-dimensional (2D) domain walls. For type- A boundaries, walls of one orientation does not affect the fluctuation of the walls of a different orientation. The results for the striped phase can be essentially carried over. For type- B boundaries, the physics is different. This is discussed in detail in Sec. II. Our results are also summarized in Table I. The speed of sound is proportional to $\sqrt{1/l}$ at both finite and zero temperatures in this case. In addition, $C(q)$ now exhibits gaplike behavior. $S(q)$ consists of a sum of two terms. One of these is Lorentzian in shape with width $1/l$; the magnitude of this peak dies off as one goes away from the phase boundary; the other is a peak of width $1/l$. The static properties such as the free energy agree with the qualitative conclusions reached by Bak *et al.* (see Ref. 1).

In Sec. III, a new issue concerning the possibility of a dislocation unbinding transition near the CIT is discussed. The magnitude of the interaction between dislocations is determined by the elastic constants of the system. These elastic constants are proportional to the sound velocity of the phonons at long wavelengths. In the commensurate phase, because of the existence of the gap in the phonon spectrum, dislocations interact with each other with a short-range potential. In the incommensurate phase, however, there now is a logarithmic part to the interaction between dislocations.

Dislocations with opposite Burger's vectors will unbind if the coefficient K of this interaction becomes small enough compared with the temperature. As the CIT is approached this coefficient goes to zero (from Table I, all the sound velocities go to zero), however. Thus we expect dislocations with opposite Burger's vectors to unbind if one is close enough to the CIT.

In the conclusion, some subtleties of the present calculations will be discussed.

II. TYPE- B TWO-DIMENSIONAL INCOMMENSURATE STRUCTURES

We wish to show that the partition function of the network of domain boundaries of type B can be related to the S matrix of an interacting electron gas with the strength of the interaction a function of the density of the domain boundaries. Even though this approach appears similar to the type- A case, there are many differences. Our main focus is the large- l limit, near the CIT. There are three equivalent ways of describing the structure in Fig. 2(b). For example, one can specify the configuration of the stripes $(A_i B_i C_i \dots)$ and then the position of the rungs $A_i A_{i+1}, C_i C_{i+1}$, etc. This is topologically the same as the configuration shown in Fig. 4 which is easier to visualize. The other two equivalent descriptions are obtained by a rotation of 120° and are also topologically the same as Fig. 4. In Fig. 4 the lengths of all the rungs in a single ladder are the same (called l_i), rungs of different ladders need not have the same lengths. The sum of all the different rung lengths, $\sum l_i$, must be equal to L_y . In Appendix B, the equivalence of these configurations is discussed in detail. If the rungs were absent, then we get back the striped phase. Because of the presence of the rungs, the fluctuation of the stripes is reduced in that they like to be more regularly spaced. However, these rungs can move horizontally so that there can be large regions with no rungs present and the fluctuation may be quite large. Note that if one has crossing domain boundaries as in Fig. 2(a) then the horizontal and vertical stripes can move independently of each other and the kind of effect that we are talking about is then absent.

One can describe the configurations of the stripes as the space-time configuration of one-dimensional quantum particles with the rungs representing the interaction between them. There are certain re-

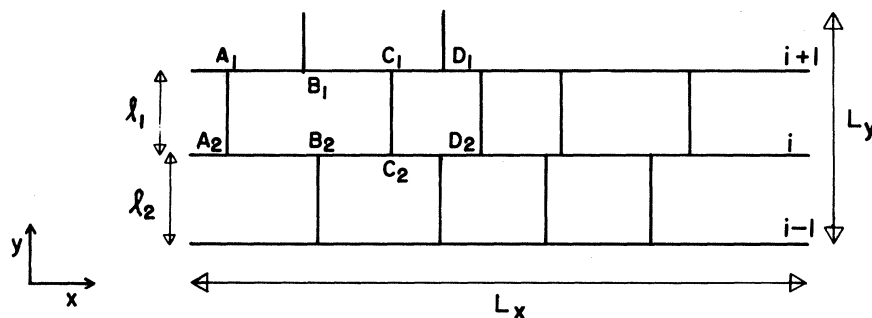


FIG. 4. Another type- B domain boundary.

restrictions on the rungs. For example: (a) in between two rungs on the same ladder, there must be rungs for the neighboring ladder; (b) the density of rungs for each ladder is the same; and (c) the rungs can bend and one has to take care of that. It turns out that these are not serious restrictions as we shall show in a moment. Now the mathematics.

For ease of presentation, let us focus on the configurations in Fig. 4. The partition function Z can be written approximately as

$$\begin{aligned} Z &= \int \prod_j dy_j S_j \\ &= \int \prod_j dy_j \int \prod_i d^2 r_i Z(\{r_i, y_j\}) \prod_{l \neq m} V(r_{lm}) \exp(\beta E_0) \\ &= \int \prod_j dy_j Z_j \end{aligned} \quad (5)$$

Where E_0 is the energy of the domain boundaries at $T=0$ (Refs. 1 and 6) $Z(\{r_i, y_j\})$ is the n -point function of the stripes such that at $T=0$, the ladders are at $\{y_j\}$. It is also the n -point function of an electron gas (Appendix A). $\prod_{i \neq j} V(r_{ij})$ is the n -point function of the rungs. The prime on the integral sign reminds us of the constraints (a) and (b) that we just mentioned. By writing the partition function in this manner, we have ignored the possibility in which the interior of the rungs can bend so that they touch the stripes as in Fig. 5. We note that the root-mean-square displacement δu of a point in the interior of a rung of length l is of the order of \sqrt{l} . In order for the process in Fig. 5 to occur δu has to be of the order of l . In the limit of large l this is not likely.

By using the notation $\prod_{i \neq j} V(r_{ij})$ we have also assumed that the interaction among the rungs in a single ladder does not produce a significant effect. This can be estimated as follows. The statistics of the rungs inside a single ladder can again be calculated using the path-integral idea with the rungs of a single ladder playing the roles of the stripes in the stripe phase (see Appendix A). The problem is mapped into that of an electron gas. In an interacting electron gas, one normally encounters an infrared divergence with the divergent parameter $\ln(E_u/E_l)$. The density of the rungs is of the order of $1/l$. This

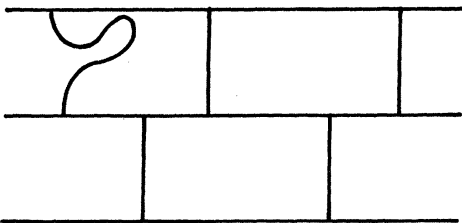


FIG. 5. This figure illustrates the possibility of bending side walls in a type-B network.

determines the Fermi energy and hence the upper-limit cutoff E_u . The lower-limit cutoff E_l is determined by the average lengths of the rungs, and is of the order of $1/l$ as well. $\ln(E_u/E_l)$ is thus of the order of unity and there is no infrared divergence. Furthermore in the low-density large- l limit, the interaction between the rungs only provide correction terms proportional to $1/l^3$ to the ground-state energy and are insignificant. $V(r_{ij})$, in the path-integral language, is then essentially the single-particle Green's function from $r_i = (y_i, t)$ to $r_j = (y_j, t' + l)$. Explicitly it is

$$V \approx \sqrt{\pi/\gamma l} \exp - (y_i - y_j)^2 / 4\gamma l [\exp(t - t')^2 \gamma \beta] \quad (6)$$

The first factor comes from the single-particle Green's function, the second, from the Boltzman factor relating the elastic energy of changing the length of a rung. Note that y becomes the time variable for the edges; hence V has a cutoff in time of the order of l . The rungs can thus be simulated by an attractive interaction keeping the walls at a distance l apart. The width of this potential is of the order of $(\beta\gamma)^{-1/2}$ [Eq. (6)]. This is very small compared with l for large l , hence it is a good approximation to replace it by a static δ function U_j of the form $U\delta(|x| - l_j)$.

We wish to identify Z with the S matrix of an electron gas. The S matrix for the interacting electron problem for imaginary time can be written as

$$S(U) = \sum_{n=0}^{\infty} (-U)^n S_n \quad (7)$$

In general, this series is dominated by a particular n value, say N . This is exactly analogous to the fact that one can describe the thermodynamics of a system either in the grand canonical ensemble by specifying the chemical potential μ ($e^{-\beta\mu} = -U$) or in the canonical ensemble by specifying the density ρ ($\rho = N/L_x L_y$). Thus

$$S \cong S' = U^N S_N \quad (8)$$

With the approximations that we have stated, $S'(U_j)$ is essentially of the form Z_j except for the constraints (a) and (b). Note that one is in general interested in $\ln Z/N$ for large N . Any constant of proportionality not diverging like $\exp(\text{const} \times N)$ is irrelevant. Hence those contributions to S' that violates (a) and (b) not on a scale of the order of N is irrelevant. Those contributions that violate (a) and (b) on a scale of the order of N corresponds to a density change in a macroscopic portion of the system. As is well known the fluctuation in density dies off as $N^{-1/2}$ where N is the number of rungs in this portion.

Our justification is now completed. The next issue is to determine the effective interaction U of the fermion system. Even though the range of U is determined by V , the magnitude of U is determined not by V but by the density of the rungs. More precisely

in the limit of large L_x , we have²

$$S = \int_{y_N > y_{N-1} > \dots > y_1} [\exp -L_x E_G(y_j)] \prod_i |\langle y_i | G(y_i) \rangle|^2 dy_i / a \quad (9)$$

where E_G is the ground-state energy of the interacting electron gas. From thermodynamics, the average number of rungs N is given by

$$N = -\frac{\partial E_G(y_j)}{\partial U_j} U_j \quad (10)$$

Equation (10) provides an implicit relationship through which U can be determined in terms of $N/L_x L_y$, the density of the rungs.

Note that the range of the potential is always the same as the interparticle spacing. Previous calculations for the interacting electron gas assumes a short-range potential and is not directly applicable here. Fortunately it is not difficult to solve for the ground state of the present problem. This is discussed in detail in Appendix C. Let us recapitulate the results here briefly. The two-particle bound-state wave function $\phi(x, l)$ is given by

$$\phi(x, l) = \begin{cases} C \sinh K |x|_{Kl}, & |x| < l \\ C e^{-K|x|}, & |x| > l \end{cases} \quad (11)$$

where

$$K = \sqrt{-\epsilon/2\beta\gamma} \quad (11a)$$

ϵ is the ground-state energy. K is related to U by the equation

$$K(1 + \coth Kl) = U/2\beta\gamma \quad (12)$$

The many-particle wave function $\psi(x_1 \dots x_N)$, in the region $x_{p1} < x_{p2} < \dots < x_{pN}$ (P is any permutation of the indices) is simply given by

$$\psi = \prod_{i=1}^{N-1} \phi(x_{pi+1} - x_{pi}, l) (-)^P \quad (13)$$

with $E_G = L_y \epsilon / l$.

That ψ is indeed the ground state comes about be-

$$S(\delta q_x + q_{x0}) \cong \frac{2\mu}{\delta q^2 + \mu^2} \exp -\frac{q_0^2 z^2}{l\mu} \left[1 - e^{-1} \cos \frac{\delta q}{\mu} \right] - \sin \frac{\delta q}{\mu} \left\{ \frac{2}{\delta q} + \frac{2\delta q}{\delta q^2 + \mu^2} \left[\frac{q_0^2 z^2}{l\mu} + \exp \left(1 - \frac{q_0^2 z^2}{l\mu} \right) \right] \right\} \quad (16)$$

where

$$\mu = lK^2 / (1 + l^2 K^2 / 2) \quad (17)$$

From Eq. (14), we know that $K = 1/(\beta\gamma la)^{1/2}$; hence $K^2 l = 1/\beta\gamma a$ and $\mu = 1/(\beta\gamma a + l/2)$. As one goes away from the CIT phase boundary, $l\mu$ decreases and the strength of the first term is reduced, the second term is basically a sharp peak of width μ .

Let us next turn our attention to the sound velocity of the epitaxial atoms due to the collective motion

cause the boundary condition is automatically satisfied (see Appendix C).

In principle, S is given by Eq. (9) for all possible distributions of the y_i 's. However, subjected to the constraint that $y_N - y_1 = L_y$, it is easy to see that (see Appendix C) $E_G(y_i)$ is a minimum (called E_G^0) when the y_i 's are uniformly distributed, and only this term dominates in the limit $L_x \rightarrow \infty$. Hence we have $S = \exp(-L_x E_G^0) |\langle y_i | G \rangle|^2$. From now on we shall therefore set $y_{i+1} - y_i = l_i = l$ in our calculation.

Combining Eqs. (11a), (12), and (10), we get the following equation:

$$4\beta\gamma K^2 (1 + \coth Kl) (1 + \coth Kl - Kl/\sinh^2 Kl)^{-1} = 1/la$$

In the limit of large l a solution of this equation is given by

$$4\beta\gamma K^2 \cong \frac{1}{(la)} \quad \text{or} \quad \epsilon = \frac{1}{2la}, \quad E_G = \frac{L_y}{2l^2 a} \quad (14)$$

Note that the partition function Z is related to S_N by

$$\begin{aligned} Z &= S_N \left(\frac{V}{U} \right)^N \exp E_0 \\ &= \exp(E_0 + L_x E_G) \left(\frac{V}{N} \right)^N \end{aligned} \quad (15)$$

Since E_0, E_G is of the order N^2 , the free energy F is just $-T(E_0 + L_x E_G)$. Note that both E_0 and E_G contains terms of the order of $1/l^2$, as has been pointed out by previous authors.¹

Because of the formation of bound states in the ground state, we expect the density autocorrelation function $C(q)$ to exhibit a gap. The structure factor $S(q)$ can also be computed by using Eqs. (2) and (3).

In Appendix C, we show that

of the domain boundaries. At zero temperature the effective elastic force between two boundaries is just $(1/l)\gamma(x-l)^2$ per unit length of the boundary. This is basically the elastic energy to compress the rungs. Thus even at $T=0$ we expect $\omega \propto \sqrt{\gamma/lq}$. We expect this result not to be changed very much for finite T since, as we have shown, the fluctuation of the "lines" is of the order of $K^{-1}(\propto \sqrt{l})$. This is still much smaller than the mean spacing l . Hence even at a finite T we expect $\omega_q \propto \sqrt{\gamma/lq}$.

III. DOMAIN-WALL MELTING

In this section, we shall discuss the possibility of a dislocation unbinding transition near the commensurate-incommensurate transition. Dislocations interact with each other with an interaction of the form

$$V = K \sum_{r \neq r'} \vec{b}(r) \cdot \vec{b}(r') \ln \frac{|r-r'|}{a} - \frac{\vec{b}(r) \cdot (\vec{r} - \vec{r}') \vec{b}(r') \cdot (\vec{r} - \vec{r}')}{|r-r'|^2}$$

It is believed that dislocations will begin to unbind at a temperature T_M related to K by $K/T_M = \pi$. K is in general a function of the elastic constants of the system. For example, for an isotropic elastic medium

$$K = \frac{4a^2\mu(\mu + \lambda)}{2\mu + \lambda},$$

where λ , μ are the Lamé coefficients. An estimate of the elastic constants can be obtained from the sound velocities since they are proportional to each other. (The interaction between the dislocations is basically due to the exchange of phonons.) Near the commensurate-incommensurate transition we expect the effective interaction between dislocations to have a logarithmic character for distances $x > l$. Furthermore, the strength of this interaction goes down as l increases. For example, for both type-*A* and type-*B* domain boundaries we expect $K \propto \gamma/l$. Hence $T_M \propto \gamma/l$. Thus at a large enough l , the dislocations would unbind. It is not clear if this has been observed experimentally.

IV. DISCUSSION

The results of this paper are already summarized in Sec. I and Table I and will not be recapitulated here. There are two minor points that we want to discuss.

The first is with regard to the structure factor, we have used the notation of the "brick-wall" model illustrated in Fig. 4, which is anisotropic. As we discussed in detail, this is basically the same as the honeycomb network, which has a higher rotational symmetry. Our structure factor should then be interpreted as corresponding to one with a wave vector along one of the symmetry directions.

The second deals with the rotation of the network of domain walls. In order to rotate the whole net-

work, a macroscopic energy is required. If this energy is negative, then the system is unstable. The energy required to rotate a part of the network is expected to be proportional to the square of the local shear. This can be absorbed in the phenomenological energy that we have used.

Note added in Proof. After this paper was submitted for publication, I noticed that J. Villain and P. Bak (report prior to publication) and Coopersmith *et al.* [Phys. Rev. Lett. **46**, 549 (1981)] have arrived at conclusions similar to those discussed in Sec. III.

APPENDIX A

In this appendix the mathematical details of the statistical mechanics of stripes will be recapitulated. There have been two treatments² that I think are basically different. Here I follow the discussion in Ref. 1 since it seems more appropriate.

The geometrical arrangement of the walls is illustrated in Fig. 1. It was discovered that this geometrical arrangement can be interpreted as the imaginary time-space trajectories of N particles. A certain elastic energy H_1 is required to bend these walls, viz.,

$$H_1 = \sum_i \gamma \int \left(\frac{dy_i}{dx} \right)^2. \quad (\text{A1})$$

This corresponds to the kinetic energy required to bend the trajectories of the particles. If the walls cannot cross then in the path-integral picture no two particles can occupy the same site. In previous treatments, to take this into account the particles are assumed to be fermions. This is not strictly correct and we will come back to it in a moment. The free energy of the two-dimensional problem becomes the ground-state energy of the fermion problem. The partition function is mapped into the S matrix with the transfer matrix mapped into the time development operator $e^{iH\delta t}$.

Mathematically, suppose at some y , the walls occupy a configuration $|x_1(y), x_2(y) \cdots\rangle$ the probability P that it will occupy a different configuration $|x'_1, x'_2 \cdots\rangle$ at $y + \delta y$ is given by the Boltzmann factor

$$\langle x'_1 \cdots | P | x_1 \cdots \rangle = \exp \left[- \sum_i (x'_i - x_i)^2 \frac{\gamma}{T} \right]. \quad (\text{A2})$$

Note that what we have written down is just the transfer matrix. The partition function Z is given by

$$Z = \int \prod_{i,j,k \cdots} dx_i(0) dx'_j(\epsilon) dx''_k(2\epsilon) \cdots \langle x(0) | P | x'(\epsilon) \rangle \langle x'(\epsilon) | P | x''(2\epsilon) \rangle \cdots \quad (\text{A3})$$

This expression is proportional to the path integral of a gas of quantum particles in one dimension as we have stated. Up to now the statistics of the particles have not been specified. To evaluate Z the largest eigenvalue of the transfer matrix P is required. P possesses the permutation symmetry. The eigenfunction of P must belong to

an irreducible representation of the permutation group S_N but it need not belong to the antisymmetric representation. The excluded volume effect can be taken into account in some other irreducible representation as well. For example, the hard-core bosons also satisfy this requirement. If only the hard core is present then both the fermions and the hard-core boson possess the same spectrum in one dimension and the above point is academic.

Note that a zero-ranged excluded volume potential between steps is easily taken into account by using fermions in this mapping. For finite-range potentials between walls, there is a "leftover" of interaction between the fermions and an interacting fermion gas is required.

This is how the power-law result for the correlation function $C(2\pi/l)$ quoted in Sec. I comes about. It is straightforward to show that in this picture the Fermi wave vector k_F of the "particles" is just π/l where l is the average spacing between the domain walls. $C(2\pi/l)$ then maps into the density correlation function at momentum transfer $2k_F$. It is known from renormalization-group-type calculations⁸ using a flat-band approximation that for a short-range interaction V between the particles, this correlation function exhibits a power-law divergence with an exponent α given by $\alpha = V/2\pi v_F$ where v_F is the Fermi velocity. Furthermore, this divergence is important only if $|q - 2k_F|/2k_F \ll 1$. Straightforward application of this result to the present problem leads to difficulties near the CIT when v_F is very small and the flat-band approximation is not applicable. Fortunately, a similar problem has been solved⁹ recently for a nearest-neighbor interaction V using the exact solutions with the Bethe ansatz and hence bypassing the flat-band approximation. From this calculation we concluded that

$$\alpha = \begin{cases} \frac{2}{\pi} \sin \pi V \left[1 - \frac{1}{l}\right] / a^2 & \text{when } V/\gamma a^2 < 1 \\ 2 - 1/\exp 2 \left[1 - \frac{1}{l}\right] & \text{when } V/\gamma a^2 \gg 1 \end{cases} . \quad (\text{A4})$$

The sound velocity mentioned in Sec. I can be obtained in the following way. Because of the anisotropic nature of the striped phase, we are talking here of the velocity of sound propagating perpendicular to the walls. (It is conceivable to have crossing stripes such that the statistical mechanics of the stripes of one orientation is independent of that of a different orientation. In that case the sound velocity may be isotropic.)

Let $u(R)$ denote deviation of the atom at R from its equilibrium position then

$$u_q = \left(\frac{\hbar}{2Mw} \right)^{1/2} (b_q^\dagger + b_{-q}) , \quad \langle u_q u_{-q} \rangle = \frac{kT}{Mw_q^2} . \quad (\text{A5})$$

$u(x)$ can also be related to the fluctuation of the domains in the long-wavelength limit since we have approximately in that case

$$u(0,y) - u(x,y) = z \int_0^x ds \delta \rho(s,y) . \quad (\text{A6})$$

The proportionality constant z is determined by the net displacement caused by a single-domain boundary. ρ is the density operator of the domain walls (and hence that of the fermion gas). From this, it is not difficult to show that

$$\langle |u_q|^2 \rangle = \frac{z}{q^2} \chi(w=0, q) , \quad (\text{A7})$$

where χ is the density response function of the electron gas. In the noninteracting case, near $q=0$ χ is given by

$$\chi_0 = \frac{1}{(\hbar^2/2m)k_F} = \frac{T}{\gamma} \frac{l}{2\pi} . \quad (\text{A8})$$

Thus

$$w_q = \frac{\sqrt{\gamma} 2\pi}{m} \frac{q}{z} . \quad (\text{A9})$$

In the presence of a short-range interaction, χ will be modified by an amount of higher order than $1/l$.

The free energy of the domain walls is proportional to the ground-state energy E_G of the fermion gas. In the absence of any interactions E_G is given by

$$E_G = \left(\frac{1}{l} \right) u_0 + \frac{\hbar^2}{2m} \frac{1}{3} \left(\frac{2\pi}{l} \right)^3 + O \left(\frac{1}{l^4} \right) , \quad (\text{A10})$$

where the first term comes from the reference energy of the fermions, the second term is just the kinetic energy. This form has been exploited to discuss the critical behavior of the CIT. One might wonder how this will be changed in the presence of any residual interaction between the fermions. A perturbation expansion in terms of this residual interaction can be written down. For any short-range interaction V , the expansion parameter is V/l so that for l large enough V/l can be quite small. Because the direct term cancels a large part of the exchange term, there are no terms proportional to $1/l^2$ and the critical behavior of the CIT remains unchanged.

APPENDIX B

Here we explain equivalence of the configurations in Fig. 2(b) to that in Fig. 4. The zero-temperature configurations have the same number of degrees of freedom. The configurations in Fig. 4 at zero temperature are specified by the vertical positions y_i of the i th straight line (edge) as well as the horizontal positions $x(i,j)$ of the j th rung between the i th and the $(i+1)$ th straight lines. The same amount of information also specifies uniquely the configurations in Fig. 2(b). This latter point is not as obvious but can be seen in the construction indicated in Fig. 6.

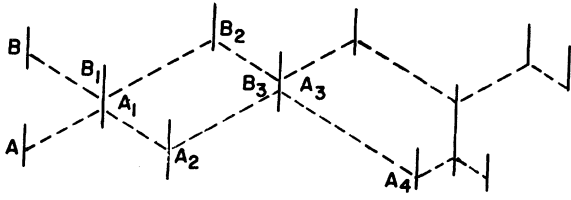


FIG. 6. An illustration showing that the configurations in Fig. 2(b) and Fig. 4 have the same number of degrees of freedom.

In this figure, we first specify the horizontal position of the rungs (indicated by the horizontal positions of the solid lines) and the initial position of the edge (indicated by A, B, \dots). The whole configuration can then be constructed from it as follows. Draw a line at 30° to the horizontal upwards from A . This intersects the next rung at A_1 . Now draw a line downwards, this intersects the next rung at A_2 and so on. Now repeat the same procedure starting at B . In this way the whole configuration is constructed.

There is one point that needs attention. If A and B are too close, then B_1 will come under A_1 and our procedure will not work. As we shall see, those configurations contribute very little to the partition function and hence are insignificant. Obviously one can specify the mean position of an edge instead of the initial position of the edge.

To establish the equivalence at a finite T , we have to show the following. Let the deviation in positions from a ground-state configuration in Figs. 4 and 2(b) be denoted symbolically by vectors $\delta\vec{r}$, $\delta\vec{r}^1$, respectively. We want to show that the mapping from $\delta\vec{r}$ to $\delta\vec{r}^1$ is one to one. Furthermore the energy measured with respect to the $T=0$ configuration corresponding to Fig. 2(a) when expressed in terms of δr should have the same functional form for that corresponding to Fig. 4. This latter condition ensures that the calculation we performed for one configuration can be directly applied to the other configuration. This energy consists of the elastic energy to bend the edges and the rungs as well as energy to stretch the rungs. It is obvious that our criterion is satisfied.

APPENDIX C

In this Appendix, the many-particle problem with the interaction $\bar{U} = U \sum_{i>j} \delta(|x_i - x_j| - l)$ will be discussed.

First let us discuss the two-body problem since, as it happens, the many-body problem is closely related to it. In the present case no two particles can sit on top of each other so that there is actually an infinitely repulsive hard core as well. In the absence of this hard core, it is well known that a bound state will form whenever the interaction is attractive. In the

presence of a hard core, there actually is a critical value of U at which binding occurs. The Hamiltonian H_2 is given by

$$H_2 = \beta\gamma(\partial_1^2 + \partial_2^2) + U\delta(|x_1 - x_2| - l) \quad (C1)$$

The solution for the bound state is, for $x > 0$

$$\phi = \begin{cases} C \sinh kx \frac{e^{-kl}}{\sinh kl}, & x < l \\ Ce^{-xk}, & x > l \end{cases} \quad (C2)$$

where $k = \sqrt{-2\epsilon\beta\gamma}$, C is a normalization constant defined by $\int \phi^2(x) dx = 1$. It is given by

$$C^2 = ke^{kl}[(\cosh kl - 1)/\sinh kl + 1]^{-1} \quad (C3)$$

Note the factor of 2 multiplying $\beta\gamma$. This is due to going to the center-of mass reference frame. From the requirement of the continuity of the logarithmic derivative, the following equation for k in terms of U is obtained

$$k(1 + \coth kl) = -U/(2\beta\gamma) \quad (C4)$$

To investigate the critical value of U for binding, take the limit $k \rightarrow 0$. We get

$$k \approx (-U/2\beta\gamma - 1/l) \quad (C5)$$

Note that k is positive. Thus no solution exists for $-U_c/2\beta\gamma < 1/l$. Note that as $l \rightarrow \infty$, $U_c \rightarrow 0$ as one would have expected from the non-hard-core result.

The mean spatial extent x is given by

$$\langle x \rangle = l \left[1 - \frac{1}{(1 + \coth kl) \sinh kl} \right]^{-1} \xrightarrow{l \rightarrow \infty} l(1 + e^{-kl}) \quad (C6)$$

As $T \rightarrow 0$, $k \rightarrow \infty$, $\langle x \rangle \rightarrow l$. The domain walls slightly expand as the temperature is increased.

Let us now focus our attention on the many-particle problem. It is not difficult to write down the ground-state wave function $\psi(x_1, \dots, x_N)$ in the region $x_{p_1} < x_{p_2} < \dots < x_{p_N}$. It is just

$$\psi = (-)^P \prod_{i=1}^{N-1} \phi(x_{p_i}, l_i) \quad (C7)$$

It is trivial to verify that ψ is indeed an eigenfunction of ψ . What makes the present problem simple is that the boundary condition is satisfied as well. Clearly there are different boundary conditions that give rise to the same spectrum in the thermodynamic limit. Here we picked one that the mean size of the system is l at $T=0$. It is obvious that our wave function satisfies this condition.

Note that because of the presence of the hard core, the binding energy is larger the larger l_i is. This is very clearly illustrated in Eq. (C5). Because of the constraint that $\sum_i l_i = L_y$, l_i cannot be infinite. Thus

we expect the binding energy to be largest when $l_i = L_y/N = l$ for all i . To illustrate, consider the limit in Eq. (C5), then $k_1 + k_2 = -U/\beta\gamma - (l_1 + l_2)/l_1 l_2$. It is obvious that for $l_1 + l_2 = 2l$, $(l_1 + l_2)/l_1 l_2 = 2l/l_1(2l - l_1)$ is largest when $l_1 = l_2 = l$. Hence $k_1 + k_2$ is largest in that case also. The general case

is more tedious to show. However, since this is physically obvious, the details will not be presented here.

Let us next calculate the structure factor of the epitaxial atom. We need to calculate $\langle \rho(u)\rho(u') \rangle$ [see Eq. (3)]. For $u > u'$, this is given by

$$\begin{aligned} \langle \rho(u)\rho(u') \rangle &= \sum_m \int \phi(u, u_1)\phi(u_1, u_2), \dots, \phi(u_m, u') \prod_{i=1}^{m-1} du_i C' u > u_1 > u_2, \dots, u' \\ &\cong \int_c \sum_m (\phi(s))^m \frac{ds}{2\pi i} e^{s(u-u')} C' . \end{aligned} \quad (C8)$$

The normalization constant C' is determined from the constraint that $\int du' \langle \rho(u)\rho(u') \rangle = N^2$. The Laplace transform $\phi(S)$ can be easily evaluated as

$$\phi(S) = \frac{C}{2} \exp(-k+S)l/(k-S) + \exp(-kl) \{ [\exp(k+S)l-1]/k + iq + [\exp(-k+S)l-1]/k-S \} / \sinh kl + \text{c.c.}$$

In the limit of large l , $\phi(S)$ is given by

$$\phi(S) = k^2/(k^2 - S^2) e^{-Sl} . \quad (C9)$$

The sum over m can be easily performed and one gets

$$\langle \rho(u)\rho(u') \rangle \cong C' \int_l^l e^{s(u-u'-l)} k^2 \frac{ds}{2\pi i} / (k^2 - S^2) \left[1 - \frac{k^2 e^{-Sl}}{k^2 - S^2} \right] . \quad (C10)$$

The integral of the right-hand side can be written as a sum of two terms, the first one is independent of $u - u'$; viz.,

$$\begin{aligned} \langle \rho(u)\rho(u') \rangle &= C' k^2 \int_l^l e^{s(u-u'-l)} \frac{ds}{2\pi i} / (k^2 - S^2 - k^2 \cosh Sl + \sinh Slk^2) \\ &\cong C' k^2 \int \frac{ds}{2\pi i} e^{s(u-u'-l)} / \left[-\frac{S^2}{2} l^2 k^2 - S^2 + Slk^2 \right] \\ &\cong C' k^2 \int \frac{dS e^{S(u-u'-l)}}{2\pi i l k^2} \left[-\frac{1}{S} + \frac{1}{S + lk^2/1 + k^2 l^2/2} \right] \\ &\cong \frac{C'}{l} \left[\int dq \frac{2 \sin q (u-u'-l)}{q} - \frac{1}{i} \int dq \frac{e^{iq(u-u'-l)}}{q + ilk^2/(1 + k^2 l^2/2)} \right] \\ &\cong \frac{C'}{l} [2\pi + 2\pi \exp[-(u-u'-l)] lk^2/(1 + k^2 l^2/2)] . \end{aligned} \quad (C11)$$

Note that in the second integral, the contour of integration is clockwise, hence the sign change. From the fact that

$$\langle \rho(u)\rho(u') \rangle \xrightarrow{u-u' \rightarrow \infty} \langle \rho(u) \rangle \langle \rho(u') \rangle \rightarrow 1/l^2 .$$

We get $C' = 1/2\pi l$. Thus for $u > u'$

$$\langle \delta\rho(u)\delta\rho(u') \rangle = \frac{1}{l^2} \exp[-(u-u'-l)] lk^2/(1 + l^2 k^2/2) \cong 1/l^2 \exp(-\mu|u-u'|) , \quad (C12)$$

where

$$\mu = lk^2/(1 + l^2 k^2/2) . \quad (C13)$$

Note that μ decreases as one approached the CIT. Hence the fluctuation in density is enhanced. $F(x)$ as is de-

finied in Eq. (3) can be easily obtained and we get

$$F(x) \approx -q_0^2 z^2 \frac{1}{l\mu} \exp(-\mu x) .$$

Substituting back into Eq. (2) we finally obtain

$$S(\delta q + q) = \int dx l^{\nu} \exp\left[-\frac{q_0^2 z^2}{l\mu} \exp(-\mu x)\right] . \quad (C14)$$

Equation (C14) can be evaluated approximately as follows. Split the region of integration into two, viz., $|\mu x| > 1$ and $|\mu x| < 1$. For $\mu x > 1$ $\exp(-x\gamma)$ is

small, we write

$$\exp\left[-\frac{q_0^2 z^2}{l\mu} \exp(-\mu x)\right] \approx 1 - \frac{q_0^2 z^2}{l\mu} \exp(-\mu x) . \quad (C15)$$

For $\mu x < 1$ μx is small, $\exp(-\mu x) \approx 1 - \mu x$, we write

$$\exp\left[-\frac{q_0^2 z^2}{l\mu} \exp(-\mu x)\right] \approx \exp\left[-\frac{q_0^2 z^2}{l\mu}\right] \exp\left[-\frac{q_0^2 z^2}{l} x\right] . \quad (C16)$$

Performing the integration, which is now trivial, we get

$$S(\delta q + q_0) = \frac{2\mu}{(\delta q)^2 + (\mu)^2} \left[\exp\left[-\frac{q_0^2 z^2}{l\mu}\right] \left(l - e^{-1} \cos \frac{\delta q}{\mu} \right) - \frac{q_0^2 z^2}{l\mu} \right] - \sin \frac{q}{\mu} \left\{ \frac{2}{\delta q} + \frac{2\delta q}{(\delta q)^2 + (\mu)^2} \left[\frac{q_0^2 z^2}{l\mu} + \exp\left[-\frac{q_0^2 z^2}{l\mu}\right] e^{-1} \right] \right\} . \quad (C17)$$

As $\rho\gamma/q_0^2 z^2$ becomes small, the approximation [in Eq. (C15)] is no longer applicable.

Only those x larger than $x_0 = (\ln q_0^2 z^2 / l\gamma) / (\delta q^2 + \gamma^2)$ contributes to the integral. For this case we get

$$S \approx 2 \frac{\sin \delta q x_0}{\delta q} - \frac{\sin \delta q x_0 2\delta q}{\delta q^2 + \gamma^2} + \frac{\cos \delta q x_0 2\gamma}{\delta q^2 + \gamma^2} . \quad (C18)$$

The first term of Eq. (C17) has now disappeared.

The evaluation of time-dependent quantities requires the knowledge of excited states which we have not investigated here. However, because of the existence of bound states for the ground states, we expect an energy gap to exist in various time-dependent density autocorrelation functions.

- ¹J. Villain, in *Ordering in Strongly Fluctuating Condensed Matter Systems*, edited by T. Riste (Plenum, New York, 1980); A. Luther, J. Timonen, and V. Pokrovsky, in *Proceedings of the Erice Summer School on Phase Transitions in Surface Films, 1979* (in press). P. Bak, D. Mukamel, J. Villain, and K. Wentowska, *Phys. Rev. B* **19**, 1610 (1979).
- ²P. G. de Gennes, *J. Chem. Phys.* **48**, 2257 (1968). Actually, the treatment by Luther *et al.* does not make use of this. However, there are gaps in all the published account of Luther's approach. They made use of a mapping into an electron-gas problem, the details of which we disagree with. See S. T. Chui and J. W. Bray, *Solid State Commun.* **32**, 1155 (1979).
- ³For the anisotropic but essentially three-dimensional compound *2H-TaSe₂*, a striped phase is reported. R. M. Flem-

- ing, D. E. Moncton, D. B. McWhan, and F. J. DiSalvo, *Phys. Rev. Lett.* **45**, 576 (1980).
- ⁴P. W. Stephens, P. Heiney, R. J. Birgeneau, and P. M. Horn, *Phys. Rev. Lett.* **43**, 47 (1979).
- ⁵V. L. Pokrovskii and A. L. Talapov, *Zh. Eksp. Teor. Fiz.* **78**, 269 (1980) [*Sov. Phys. JETP* **51**, 134 (1980)]; H. J. Schulz (unpublished); T. Nattermann (unpublished).
- ⁶The most detailed calculation is by H. Shiba, *Tech. Rep. I.S.S.P.* **1**, 940 (1978).
- ⁷F. C. Frank and J. H. Van der Merwe, *Proc. R. Soc. London* **198**, 205 (1949); S. C. Ying, *Phys. Rev. B* **3**, 4160 (1971).
- ⁸See, for example, Yu A. Bychkov, L. P. Gorkov, and I. E. Dzyaloshinskii, *Sov. Phys. JETP* **23**, 489 (1966).
- ⁹S. T. Chui (unpublished).